Appl. Phys. B (2013) 113:485–490
DOI 10.1007/s00340-013-5486-2

Applied Physics B
Lasers and Optics

Femtosecond laser-induced nanostructure-covered large-scale waves on metals

Taek Yong Hwang · Chunlei Guo

Published online: 24 May 2013

Abstract Through femtosecond (fs) laser pulse irradiation (pulse duration: 65 fs, central wavelength: 800 nm, and repetition rate: 250 Hz), we investigate the morphological evolution of fs laser-induced periodic surface structure on Au and Pt, called a nanostructure-covered large-scale wave (NC-LSW) with a period of tens of microns, densely covered by iterating stripe patterns of nanostructures and microstructures. We show that the surface morphology of NC-LSW crucially depends on the fluence of the laser, the number of irradiating pulses, and the incident beam angle. Our experimental observations allow us to establish a three-step model for the NC-LSW formation: the formation of laser-induced surface unevenness, inhomogeneous energy deposition due to the interference between the incident light and the scattered field, and nonuniform energy deposition due to shielding by the peaks of LSW.

1 Introduction

Laser-induced periodic surface structure (LIPSS) has been extensively studied in a variety of materials including semiconductors, metals, and dielectrics using cw and relatively long-pulsed lasers [1–7]. Based on the previous studies, the formation mechanisms of LIPSS generated by cw and relatively long-pulsed lasers are currently well understood. Depending on the fluence of laser, the formation of LIPSS is attributed to either the interference between the incident light and the generated surface electromagnetic wave or the laser-induced capillary wave [3–7]. However, recent studies on LIPSS showed that the period of LIPSS induced by femtosecond (fs) laser deviates significantly from a period predicted from the two well-known mechanisms, and this deviation has triggered extensive studies on the LIPSS with fs laser pulses [8–24]. To explain this deviation, many different mechanisms have been suggested in the past decade such as the transient change in the optical properties of surface [23, 24], self-organization [14, 19], the parametric decay of laser light to surface plasmons [12], and the change of optical properties of surface due to surface nanostructures [11]; however, the formation mechanism of fs LIPSS is still under debate in the literature. Most of the previous studies have been limited to a decreased period compared to the period of regular LIPSS [8–14, 18, 21–24]. However, in more recent studies by us, we demonstrated the formation of a new type of LIPSS, called a nanostructure-covered large-scale wave (NC-LSW) with a longer period than the period of regular LIPSS at relatively large incident angles [15, 16, 20].

In this work, following *p*- and *s*-polarized femtosecond (fs) laser pulse irradiation, we produce a new type of laser-induced periodic surface structure on Au and Pt, namely NC-LSW with a period on the order of tens of microns, densely covered by an iterating pattern consisting of stripes of nanoscale and microscale structures. We show that the period of NC-LSW can be controlled by the fluence of laser, the number of laser pulses, and the incident angle of the fs laser pulses.

2 Experimental

The laser used in our experiment is an amplified Ti:sapphire fs laser system that generates 65-fs pulses with an

T. Y. Hwang · C. Guo (✉)
The Institute of Optics, University of Rochester, Rochester, NY 14627, USA
e-mail: guo@optics.rochester.edu

energy of 1 mJ/pulse, and it operates with a 250 Hz repetition rate at a central wavelength of 800 nm. The samples used in our experiment are Au and Pt foils with a thickness of 0.5 mm and are prepared by mechanically polishing the surfaces with 0.1-μm-grade aluminum oxide powder. To produce surface structures, a train of *p*- or *s*-polarized fs laser beam is weakly focused onto the sample surface using a lens with a focal length of 250 mm. We produced NC-LSW at incident angles (θ) between 50° and 75° with a resolution of 1°. The major and minor 1/e intensity radii of the elliptical laser spot on the samples are used to calculate laser fluence. The number of pulses in a pulse train is controlled by an electromechanical shutter. The pulses are negatively chirped at the output of the amplifier to pre-compensate for the dispersion of all the optics prior to interacting with metals. All experiments are performed in ambient air, and the surface texture and three-dimensional morphological profile of laser-treated Au and Pt are studied with a scanning electron microscope (SEM) and a UV laser-scanning confocal microscope (UV-LSCM) following fs laser pulse irradiation. The propagation direction and polarization of the laser beam are marked in the figures with a single-headed and a double-headed arrow, respectively. The error bars shown in the Figs. 1d, 2, 4, and 5 indicate the standard deviation of the period of NC-LSW.

3 Results and discussion

When an Au surface is irradiated by a train of 1,000 *p*-polarized laser pulses with fluences of 0.26, 0.39, and 0.48 J/cm^2 at an incident angle of 70°, the upper part of the central region of the modified surface is covered with a NC-LSW, as shown in Fig. 1a–c. The period of NC-LSW is much longer than the predicted period by the well-known interference mechanism, ~10 μm, as shown in Fig. 1d. We also systematically measure the dependence of the NC-LSW period on the laser fluence in Fig. 1d. As shown in Fig. 1d, we can clearly see that the period of NC-LSW increases continuously with the laser fluence, and the curvature of each LSW also tends to increase with laser fluence until the structures start to disappear above a fluence of 0.52 J/cm^2. Moreover, for NC-LSW as shown in Fig. 1a–c, the period is larger in the center than at the edge, again indicating the period is larger in a higher laser fluence region.

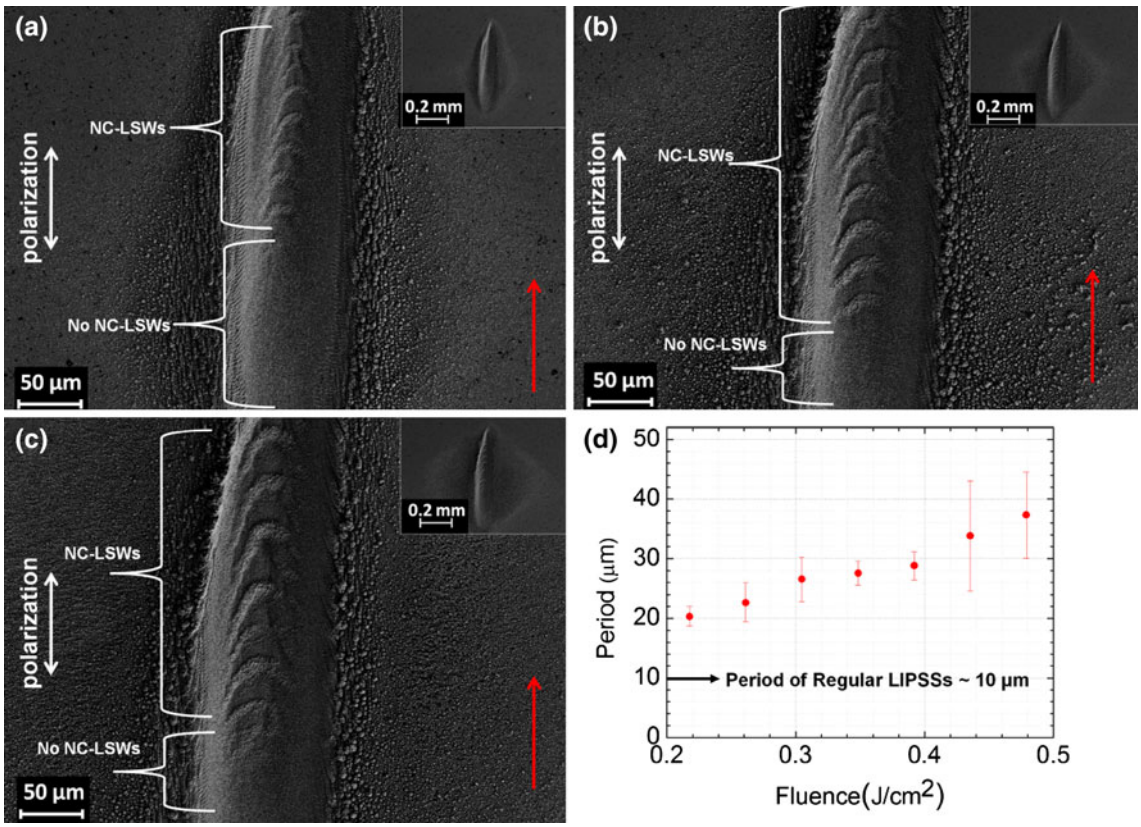

Fig. 1 SEM images of the modified Au surface following 1,000-pulse irradiation with different laser fluence (F) at an incident angle of 70°. The NC-LSW only appears in the *upper part* of the central region of the modified surface at **a** $F = 0.26$ J/cm^2, **b** $F = 0.39$ J/cm^2, and **c** $F = 0.48$ J/cm^2. Dependence of the period of NC-LSW on the laser fluence is shown in (**d**). The insets in **a**–**c** are the overview of the modified Au surfaces

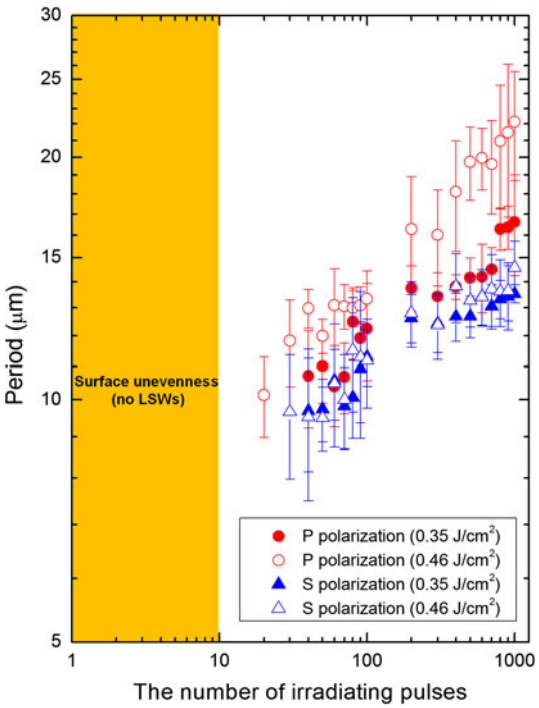

Fig. 2 Dependence of NC-LSW period on the number of irradiating *p*- and *s*-polarized fs pulses with fluences of 0.35 and 0.46 J/cm^2

Next, we study the dependence of the NC-LSW period on the number of irradiating pulses following *p*- and *s*-polarized fs pulse irradiation with a fluence of 0.35 or 0.46 J/cm^2 at an incident angle of 70°. The results of this dependence are plotted in Figs. 2 and 3. Under our experimental condition, following a few pulses, we can only see surface unevenness including both the initial surface roughness and the small nonperiodic surface structures induced by the laser pulses. This unevenness is the onset of the NC-LSW formation. Consistent with our previous study on Au [15], the NC-LSW is produced on Pt with *p*-polarized pulse irradiation with continued irradiation, and its period continuously increases with the number of pulses and the laser fluence. We also show that the NC-LSW can be induced using *s*-polarized laser pulse irradiation, as shown in Fig. 2. Moreover, as can be seen in Fig. 2, the period of NC-LSW with s polarization is similar to that with p polarization at low pulse numbers; however, unlike the p polarization, the NC-LSW period with s polarization increases slowly with the number of irradiating pulses.

Figure 3 shows the surface morphology of NC-LSW induced by *s*-polarized pulse irradiation at an incident angle of 70°. The NC-LSW induced by *s*-polarized fs pulse irradiation is also densely covered with an iterating pattern

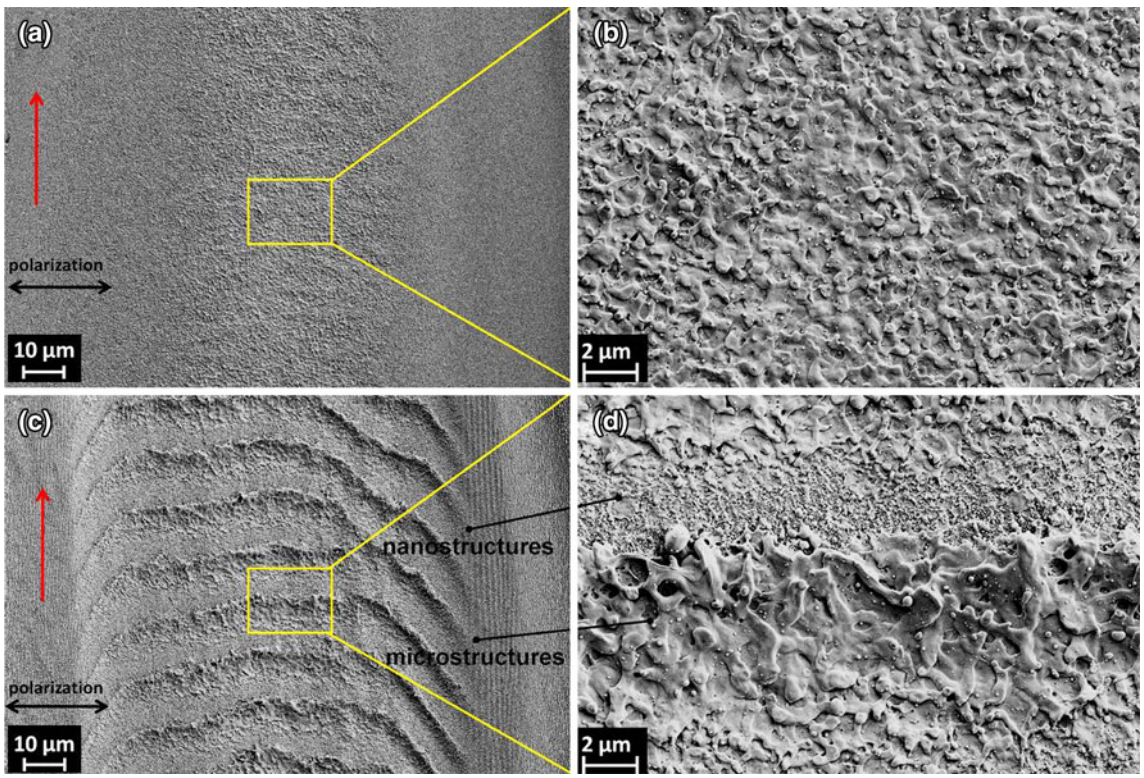

Fig. 3 SEM images of modified Pt surface following 30 *s*-polarized pulses [(**a**), (**b**)] and 1,000 *s*-polarized pulses [(**c**), (**d**)] with a fluence of 0.35 J/cm^2 at an incident angle of 70°

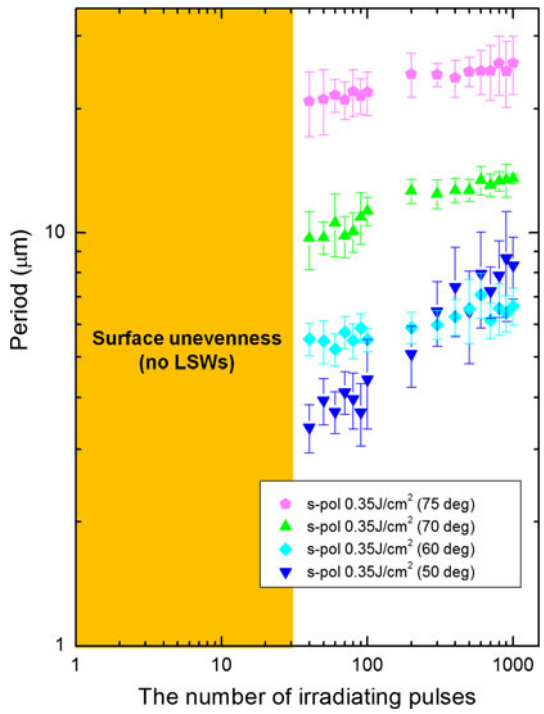

Fig. 4 Incident angle dependence of the NC-LSW period as a function of the number of irradiating pulses at a fluence of 0.35 J/cm^2

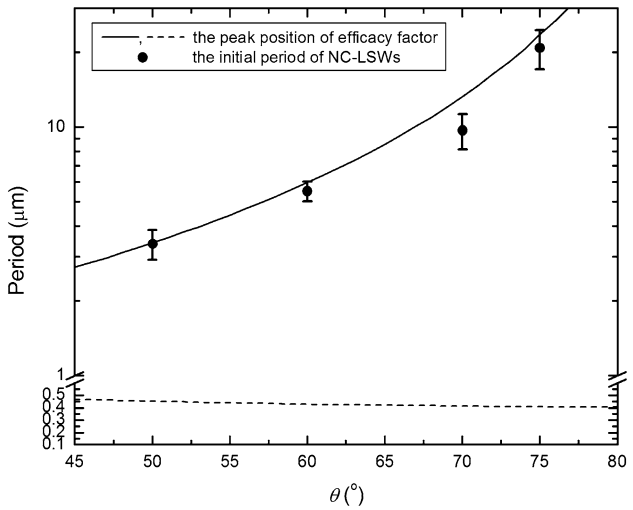

Fig. 5 Predicted periods on Pt based on the theory of efficacy factor are indicated with the *solid and dashed lines*. Observed NC-LSW periods at low pulse numbers are clearly satisfied with the *solid line* from the efficacy model. The dielectric constant of Pt used here is $-15.5 + 23.5\,i$ (Ref. [26])

that consists of stripe patterns of nanoscale and microscale surface structures, similar to what we have seen for *p* polarization on Au in Ref. [15]. This iterating pattern is initially invisible before the clear formation of large-scale wave; however, once the LSW is formed, this pattern becomes much clearer with more pulse irradiation as shown in Fig. 3b and d.

As mentioned earlier, surface unevenness including both the initial surface roughness and the small randomly oriented nanoscale surface structures induced by the laser pulses can be only seen following a few pulses. This unevenness is the onset of the formation of NC-LSW, and we expect that this can allow the light to be scattered at the surface. To verify if the scattered field plays an important role in the formation of NC-LSW, we consider the so-called efficacy factor that shows a given wave vector value of laser-induced periodic surface structures as a function of incident angle and polarization of light with the shape (*s*) and filling factor (*f*), describing the properties of surface roughness [4]. Based on the theory of efficacy factor, laser-induced periodic surface structures are most likely formed when the wave vectors of the induced surface field correspond to the peaks of efficacy factor, which also correspond to the Fourier components of inhomogeneous energy deposition owing to the interference between the incident light and the scattered field [4]. In case of p polarization, the wave vectors of the inhomogeneous energy deposition on metals correspond to those from the interference between surface plasmons and the incident laser beam [4, 18, 23].

We control the incident angle of *s*-polarized fs laser beam at incident angles of 50°, 60°, 70°, and 75° as shown in Fig. 4. S polarization is chosen because the peak positions of the efficacy factor are almost independent of the shape and filling factor, which are generally unknown parameters [2, 4]. The peak positions also satisfactorily predict the period of laser-induced surface structures even at a larger incident angle [2, 4]. As seen from Fig. 4, the initial period of NC-LSW following about 40 laser pulses shows the significant dependence on the incident beam angle, and the NC-LSW period at each incident angle further increases with continued irradiation.

The calculated peak positions for Pt based on the efficacy factor as a function of the incident beam angle are shown in Fig. 5. For off-normal incidence, two peaks usually exist on the efficacy factor, and these two peak positions at each θ correspond to the periods of LIPSS, indicated by the solid and dashed lines in Fig. 5. As shown in Fig. 5, the initial periods of NC-LSW following 40-pulse irradiation are satisfactorily predicted by the solid line that increases with θ. This indicates that the scattered field eventually plays a decisive role in determining the initial period by depositing energy inhomogeneously through interfering the scattered field with the incident light. We note that another peak of efficacy factor described as the dashed line in Fig. 5 is not observed in our experiment. We believe that the size of randomly oriented surface structures, initially formed, is large enough to smear the surface structures less than half a micrometer, as shown in Fig. 3b. Although this inhomogeneous energy deposition due to the

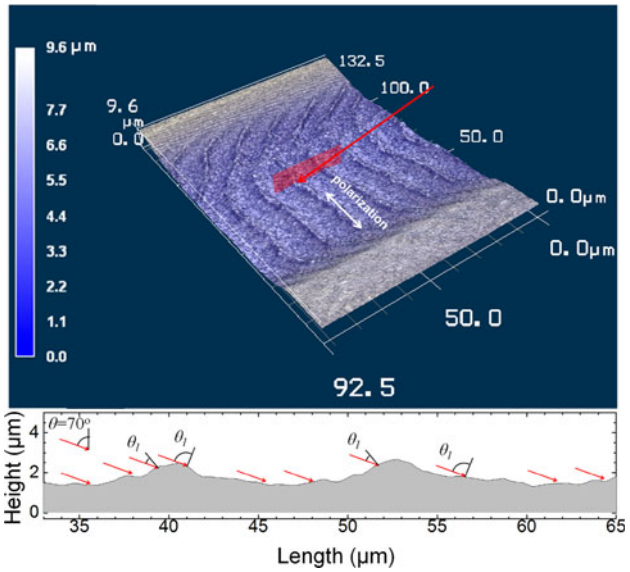

Fig. 6 UV-LSCM image of NC-LSW following 1,000 *s*-polarized pulse irradiation with a fluence of 0.35 J/cm^2 at an incident angle of 70°

interference successfully describes the initial period of NC-LSW, the inhomogeneous energy deposition cannot explain the increase in the NC-LSW period with the number of irradiating pulses and the laser fluence shown in Figs. 1 and 2. Therefore, at this stage, other factors need to be considered to understand underlying mechanisms increasing the NC-LSW period.

Once the LSW is initiated, as shown in Fig. 6, the peaks of the LSW can partially shield the surface from laser irradiation and can change the incident angle at the surface in a periodic pattern, because the laser beam has a large incident angle. Also, over the period of each large-scale wave, the absorbed energy per surface area changes at different points because the incident beam angle (θ_l) continuously changes across the large-scale wave period, as shown in Fig. 6. Therefore, the metal surface will be heated periodically by pulse irradiation, and this nonuniform periodic heating can generate a periodic distribution of the size of randomly oriented nanostructures superimposed on the LSW. Contrasted with the period of LIPSS induced by fs pulses [11, 18], the size of randomly oriented surface structures on metals is larger with higher laser fluence and a larger number of laser pulses [25]. In Fig. 3b, the size of the randomly oriented surface structures is nearly uniform on the Pt surface along the plane of incidence before the formation of LSW, indicating uniform irradiation on the Pt surface. However, once the LSW is formed, the size of the randomly oriented surface structures superimposed on the LSW shows a periodic modulation along the grating vector of NC-LSW, as shown in Fig. 3d. This observation leads us to believe that the nonuniform periodic heating plays a key role in forming a NC-LSW on metals.

This nonuniform periodic heating due to the peaks of NC-LSW can be understood by considering the absorbed energy per normalized surface area and per pulse energy (AESP) [22] that is proportional to the absorbed laser fluence at a local point of the surface, because the morphological evolution of laser-induced surface structures should be closely related to the heating of the surface [22]. To see how the incident angle at the surface of the structures (θ_l) affects the surface heating on metal surfaces following fs pulse irradiation, we calculate the AESP as a function of θ_l by assuming no resonant absorption is involved. The AESP can be defined as the following equation: [22]

$$\mathrm{AESP} = \frac{E_a A(\theta_l = 0^\circ)}{E_i A(\theta_l)} = [1 - R_f(\theta_l)] \cos\theta_l$$

where E_i is the input pulse energy, E_a is the absorbed pulse energy, $A(\theta_l)$ and $R_f(\theta_l)$ are the surface area and the Fresnel reflection of the surface at the incident angle at the surface of structures (θ_l), respectively, and the normalized surface area is defined as $A(\theta_l)/A(\theta_l = 0)$.

Based on the AESP versus θ_l plot in Fig. 7, the AESP on Au and Pt continuously decreases with θ_l regardless of the polarization of the laser beam. This directly indicates that the absorbed laser fluence will be higher on the surface facing toward the laser beam irradiation (S_t) than on the surface facing away from the laser beam irradiation (S_a) because of a smaller AESP due to a larger θ_l. This nonuniform periodic heating eventually increases the amplitude of NC-LSW by ablating a larger amount of material on S_t than on S_a and by transferring liquid metals toward the crests of the LSW due to the recoil pressure induced by laser ablation. This eventually results in increasing the period of nonuniform periodic heating because a larger

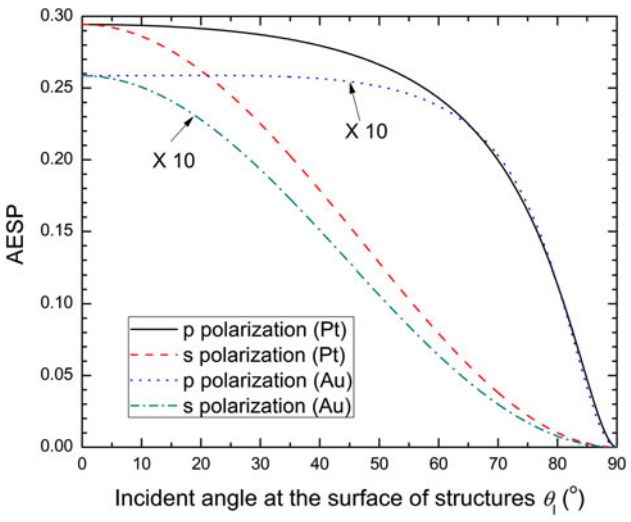

Fig. 7 Absorbed energy per normalized surface area per pulse energy (AESP) versus the incident angle at the surface of structures. The AESP on Au is scaled up by ten times

area will be shielded by the peak of LSW. Therefore, by repeating this process through continued irradiation, the period and height of NC-LSW are continuously increased. This is also explains another observation in our experiments: the period of the NC-LSW increases with the laser fluence, because higher laser fluence will enhance NC-LSW growth during each pulse irradiation.

4 Conclusion

In conclusion, by using fs laser pulse irradiation, we investigate the morphological evolution of fs laser-induced periodic surface structure, called NC-LSW with a period of tens of microns, densely covered by iterating stripe patterns of nanostructures and microstructures. We show that the surface morphology of NC-LSW crucially depends on the fluence of the laser, the number of irradiating pulses, and the incident beam angle. Our experimental observation allows us to establish a three-step model for the NC-LSW formation: the formation of laser-induced surface unevenness, inhomogeneous energy deposition due to the interference between the incident light and the scattered field, and nonuniform energy deposition due to shielding by the peaks of LSW.

Acknowledgments This work was supported by the US Air Force Office of Scientific Research.

References

1. M. Birnbaum, J. Appl. Phys. **36**, 3688 (1965)
2. S.E. Clark, D.C. Emmony, Phys. Rev. B **40**, 2031 (1989)
3. J.F. Young, J.E. Sipe, H.M. van Driel, Phys. Rev. B **30**, 2001 (1984)
4. J.E. Sipe, J.F. Young, J.S. Preston, H.M. van Driel, Phys. Rev. B **27**, 1141 (1983)
5. A.M. Bonch-Bruevich, M.N. Libenson, V.S. Makin, V.V. Trubaev, Opt. Eng. **31**, 718 (1992)
6. W.D. Liu, L.M. Ye, K.X. Liu, J. Appl. Phys. **109**, 043109 (2011)
7. Z. Guosheng, P.M. Fauchet, A.E. Siegman, Phys. Rev. B **26**, 5366 (1982)
8. L. Qi, K. Nishii, Y. Namba, Opt. Lett. **34**, 1846 (2009)
9. T.Q. Jia, H.X. Chen, M. Huang, F.L. Zhao, J.R. Qiu, R.X. Li, Z.Z. Xu, X.K. He, J. Zhang, H. Kuroda, Phys. Rev. B **72**, 125429 (2005)
10. Y. Shimotsuma, P.G. Kazansky, J. Qiu, K. Hirao, Phys. Rev. Lett. **91**, 247405 (2003)
11. A.Y. Vorobyev, V.S. Makin, C. Guo, J. Appl. Phys. **101**, 034903 (2007)
12. S. Sakabe, M. Hashida, S. Tokita, S. Namba, K. Okamuro, Phys. Rev. B **79**, 033409 (2009)
13. J. Bonse, M. Munz, H. Sturm, J. Appl. Phys. **97**, 013538 (2005)
14. J. Reif, F. Costache, M. Henyk, S.V. Pandelov, Appl. Surf. Sci. **197–198**, 891 (2002)
15. T.Y. Hwang, C. Guo, J. Appl. Phys. **109**, 083521 (2011)
16. T.Y. Hwang, C. Guo, J. Appl. Phys. **110**, 073521 (2011)
17. Y. Shimotsuma, M. Sakakura, P.G. Kazansky, M. Beresna, J. Qiu, K. Miura, K. Hirao, Adv. Mater. **22**, 4039 (2010)
18. J.P. Colombier, F. Garrelie, N. Faure, S. Reynaud, M. Bounhalli, E. Audouard, R. Stoian, F. Pigeon, J. Appl. Phys. **111**, 024902 (2012)
19. J. Reif, O. Varlamova, S. Varlamov, M. Bestehorn, Appl. Phys. A **104**, 969–973 (2011)
20. T.Y. Hwang, C. Guo, Appl. Phys. Lett. **101**, 021901 (2012)
21. G. Miyaji, K. Miyazaki, J. Laser Micro/Nanoeng. **5**, 86 (2010)
22. T.Y. Hwang, C. Guo, Opt. Lett. **36**, 2575 (2011)
23. F. Garrelie, J.P. Colombier, F. Pigeon, S. Tonchev, N. Faure, M. Bounhalli, S. Reynaud, O. Parriaux, Opt. Express **19**, 9035 (2011)
24. D. Dufft, A. Rosenfeld, S.K. Das, R. Grunwald, J. Bonse, J. Appl. Phys. **105**, 034908 (2009)
25. A.Y. Vorobyev, C. Guo, Opt. Express **14**, 2164 (2006)
26. M.A. Ordal, L.L. Long, R.J. Bell, S.E. Bell, R.R. Bell, J.R.W. Alexander, C.A. Ward, Appl. Opt. **22**, 1099 (1983)